

EBEX - The E and B Experiment

Will Grainger¹, Asad M. Aboobaker², Peter Ade³, François Aubin⁴, Carlo Baccigalupi⁵, Eric Bissonnette⁴, Julian Borrill^{6, 7}, Matt Dobbs⁴, Shaul Hanany², Clayton Hogen-Chin², Johannes Hubmayr², Andrew Jaffe⁸, Bradley Johnson⁹, Terry Jones², Jeff Klein², Andrei Korotkov¹⁰, Sam Leach⁵, Adrian Lee¹¹, Lorne Levinson¹², Michele Limon¹, John Macaluso¹⁰, Kevin MacDermid⁴, Tomotake Matsumura¹³, Xiaofan Meng¹¹, Amber Miller¹, Michael Milligan², Enzo Pascale³, Dan Polsgrove², Nicolas Ponthieu¹⁴, Britt Reichborn-Kjennerud¹, Tom Renbarger¹⁵, Ilan Sagiv², Federico Stivoli⁵, Radek Stompor¹⁶, Huan Tran⁷, Greg Tucker¹⁰, Jerry Vinokurov¹⁰, Matias Zaldarriaga¹⁷, Kyle Zilic²

¹*Columbia University, New York, NY 10027,*

²*University of Minnesota School of Physics and Astronomy, Minneapolis, MN 55455,*

³*Cardiff University, Cardiff, CF24 3AA, United Kingdom,*

⁴*McGill University, Montréal, Quebec, H3A 2T8, Canada,*

⁵*Scuola Internazionale Superiore di Studi Avanzati, Trieste 34014, Italy,*

⁶*National Energy Research Supercomputing Center, Lawrence Berkeley National Laboratory,*

⁷*University of California, Berkeley, Space Sciences Lab, Berkeley, CA 94720,*

⁸*Imperial College, London, United Kingdom,*

⁹*Oxford University, Oxford, OX1 3RH, England, United Kingdom,*

¹⁰*Brown University, Providence, RI 02912,*

¹¹*University of California, Berkeley, Berkeley, CA 94720,*

¹²*Weizmann Institute of Science, Rehovot 76100, Israel,*

¹³*California Institute of Technology, Pasadena, CA 91125,*

¹⁴*Institut d'Astrophysique Spatiale, Université Paris-Sud, Orsay, 91405, France,*

¹⁵*University of California, San Diego,*

¹⁶*Laboratoire Astroparticule et Cosmologie (APC), Université Paris Diderot, Paris Cedex 13, 75205, France,*

¹⁷*Harvard University Center for Astrophysics, Cambridge, MA 02138*

Abstract

The E and B Experiment (*EBEX*) is a CMB polarization experiment designed to detect or set upper limits on the signature of primordial gravity waves, measure E-mode polarization and measure the B-mode lensing signal. *EBEX* has sufficient sensitivity to set an upper limit at 95% confidence on the tensor to scalar ratio < 0.02 . In addition, *EBEX* will carry out multi-frequency, high resolution mapping of the polarized foreground emission from thermal dust. This article reviews our strategy for achieving our science goals and discusses the experiment.

1 Introduction

The paradigm of inflation^{1,2,3,4}, in which the Universe underwent exponential expansion within its first $\sim 10^{-35}$ sec, is consistent with all current astrophysical measurements^{2,6}. It is the leading model of the state of the Universe at early times that convincingly explains otherwise puzzling cosmological phenomena⁷. However, many of the details of the inflationary scenario are uncertain, and the paradigm currently lacks any strong confirmation. Inflation predicts a stochastic background of gravity waves, the inflationary gravity wave background (IGB)^{8,9,10,11,12}. The amplitude of the IGB is predicted to be proportional to the energy scale of inflation, $V^{1/4}$, via $V^{1/4} = 3.7 \times 10^{16} (T/S)^{1/4}$ GeV, where $T/S = C_2^{GW}/C_2^S$ is the ratio of the temperature quadrupoles produced by gravity waves and by density perturbations, and V is the inflaton potential. The current 2σ upper limit⁵ of $T/S \approx 0.2$ implies $V^{1/4} < 2.5 \times 10^{16}$ GeV.

The best known way to search for the IGB is through its signature on the Cosmic Microwave Background (CMB) polarization^{13,14}. Primordial energy density perturbations produce a curl-free ('E-mode') polarization pattern. The IGB produces both an E-mode and a curl ('B-mode') pattern of polarization vectors that density perturbations alone cannot

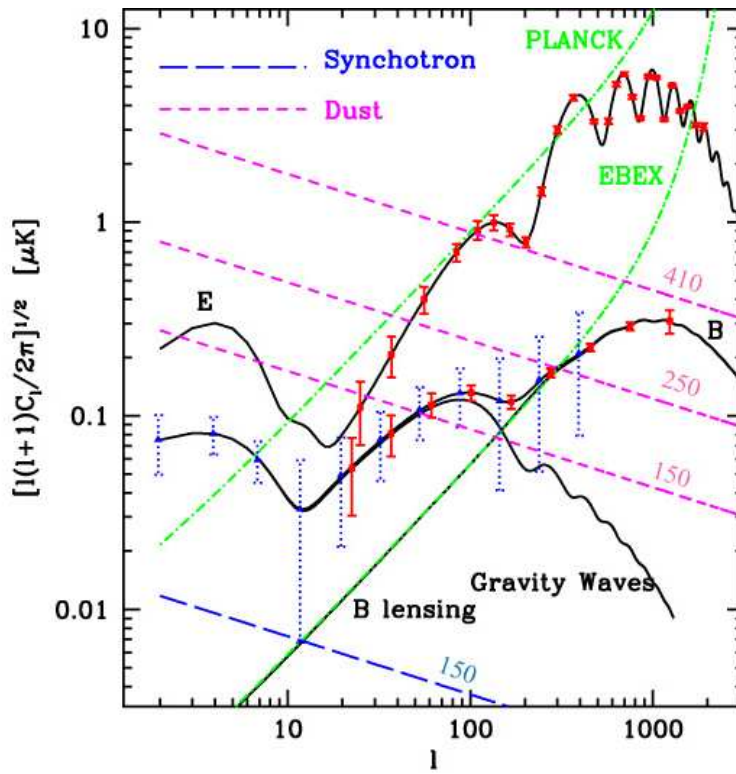


Figure 1: The power spectra for B and E-modes for a $T/S = 0.1$ Λ CDM universe (black lines), with predicted instrumental noise and cosmic variance error bars for *EBEX* (red) and Planck 1 year (blue). The upper black line, labeled ‘E’, is the E-mode, and ‘B’ is the B-mode signal, which comes from both the lensing signal and IGB (labeled ‘Gravity waves’). Also shown is a model of expected dust and synchrotron signal levels in our frequency bands and within the LD sky patch. Finally, the power spectra of pixel noise (green) are shown for both Planck and *EBEX*.

produce^{15,16}. The amplitude of the B-mode signal is related to the energy scale of inflation by $V^{1/4} = 2 \times 10^{16} (B_{\text{peak}}/0.1\mu\text{K})^{1/2}$ GeV where B_{peak} is the amplitude of the power spectrum of the B-mode in μK at $l = 90$.

The E and B Experiment (*EBEX*) is a balloon borne CMB polarization experiment designed to observe the E and B-mode polarization. It is due for a test launch from Fort Sumner, New Mexico in September 2008, and a long duration (LD) balloon flight in the 2010 from McMurdo base, Antarctica. In this paper we will outline our science goals and discuss the experimental details of how this measurement will be performed.

2 Science goals

EBEX has a number of CMB science goals, which we will enumerate while referencing Figure 1.

Detect or set an upper limit on the IGB signal. The lower curve of Figure 1, labeled Gravity Waves, shows the IGB power spectrum of the CMB in a standard Λ CDM cosmology for a tensor to scalar ratio $T/S = 0.1$. The red error bars show the expected 1σ determination of the overall B-mode for a 14 day *EBEX* LD flight. If the T/S ratio is close to 0.1, *EBEX* will detect the IGB signal and thus determine the energy scale of inflation. If the B-mode signal is not detected, we will put a 2σ upper limit on $T/S < 0.02$, corresponding to an energy scale of 1.4×10^{16} GeV. This would rule out so-called ‘classic inflationary’ models, often considered the simplest models of inflation¹⁸.

Make a cosmic-variance limited measurement of the E-mode CMB power spectrum. *EBEX* will make cosmic variance limited measurements of the E-mode spectrum from $25 < l < 1500$. These measurements will improve the accuracy of determination of

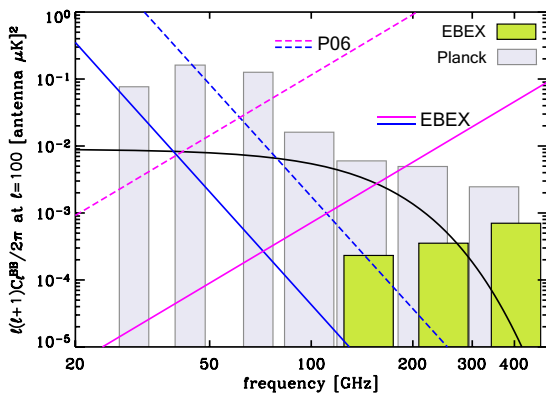


Figure 2: Spectrum of B-mode foregrounds from Galactic dust (magenta) and synchrotron (blue) expected outside of WMAP’s P06 mask (dashed) and our estimate in the *EBEX* area (solid), and the B-mode CMB (black), all at $l = 100$. The *EBEX* (green histograms) and Planck noise (light gray histograms) levels in their respective frequency bands are also shown.

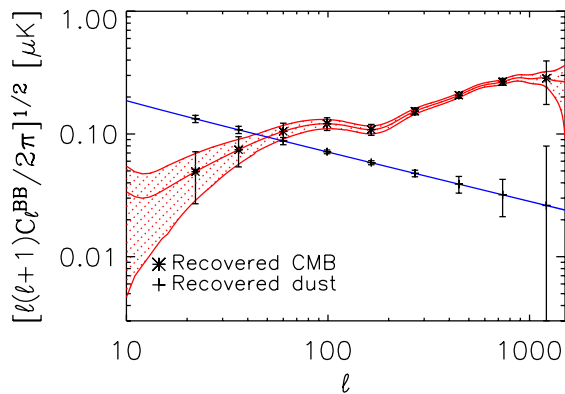


Figure 3: B-mode signal reconstruction with dust correction. The input CMB B-mode power spectrum (solid red), and calculated power spectrum of the simulated dust map (solid blue) are shown. The results of 10 map domain simulations (that include instrumental noise) of the reconstruction of the CMB (black crosses) and dust (black squares) are shown with errors. The overall increase in the errors over the majority of the l range is small.

cosmological parameters.

Measure the B-mode CMB lensing signal. Gravitational lensing of CMB photons along the line of sight by large-scale structures in the Universe distorts the E-mode polarization, modifies its power spectrum¹⁹ and creates a B-mode polarization even if gravity waves are not present²⁰. The curve labeled ‘B’ on Figure 1 shows the combined B-mode spectrum from both the IGB and lensing, and the curve ‘B lensing’ shows the lensing alone. Currently the amplitude of the lensing B-mode signal is predicted to within $\approx 20\%$ ^{21,22} (from existing large scale structure and E-mode measurements). *EBEX* is designed to detect and constrain the amplitude of this component with an accuracy of $\approx 7\%$.

Characterize the polarized dust emission in both E and B-mode polarizations. CMB measurements have three primary sources of contaminating foreground emission: dust, synchrotron, and extra-galactic point-sources. A plot of the dust and synchrotron power spectra is shown in Figure 2. In the low foreground area selected for the LD flight, synchrotron is expected to be sub-dominant at 150 GHz and even less significant at higher frequencies. However, the signal level from dust is expected to be comparable to the cosmological signal at 150 GHz, and larger at higher frequencies. With three frequencies centered on 150, 250 and 410 GHz, and 752, 376 and 278 detectors in those bands, respectively, simulations show that *EBEX* should have the sensitivity to subtract the dust foreground and reconstruct the power spectrum of the B-mode, with only a small increase in uncertainty; see Figure 3. To calculate the results in this Figure we produced ten realizations of CMB B-mode, dust signal and instrumental noise. Using a parametric approach²⁵ we estimated both the dust and CMB signal and assessed the additional error on the reconstruction of the CMB signal coming from this simultaneous estimate. We find that for $\ell < 900$ the increase in error is less than 30% compared to the error coming from instrumental noise and sample variance.

3 Scan strategy

The range of angular scales we have chosen to probe sets both the resolution (and hence beam size of the instrument) and the size of the sky patch we scan. Figure 1 shows the expected measurement achievable with a 14 day flight (the average for LD⁷) and 752 150 GHz detectors if we observe 350 square degrees of sky. The scan strategy is to perform a sawtooth scan in azimuth stepping in elevation after 4 scans. Scanning in azimuth ensures uniform atmospheric loading. The scan speed is 0.7 sec, and the amplitude of the sawtooth is 17 degrees. After the elevation has changed by 10 degrees in declination the sequence is restarted. This scan

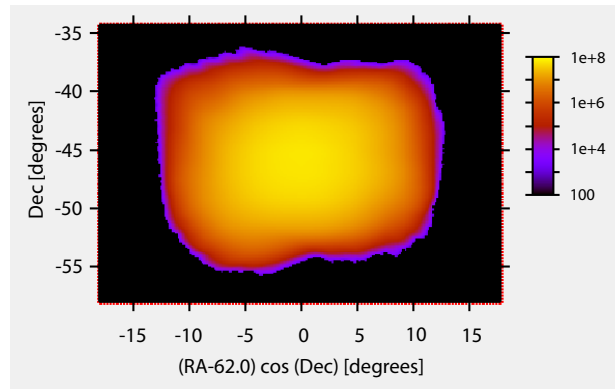


Figure 4: Detector sample counts for *EBEX* in our LD sky patch. The count is for the 752 150 GHz detectors and a 14 day flight.

strategy provides re-visitation of pixels on multiple timescales and with different orientation between the instrument and fixed coordinates on the sky (i.e. cross-linking). Both of these are important for minimizing instrumental systematics. The sky coverage achieved is shown in Figure 4.

4 Experimental implementation

The experimental platform is shown in Figure 5. The inner frame holds the optics, cryostat, readout and power crates, gyroscopes and star cameras. The outer frame holds the rest of the attitude control system electronics (sun sensor, magnetometer, tiltmeters), flight computer, reaction wheel, and Columbia Scientific Balloon Facility’s flight support electronics. The azimuth attitude is controlled by modulating the acceleration of the reaction wheel, and a motor in the rotator allows torque to be applied against the flight-line to prevent the reaction wheel saturating. The elevation between the inner and outer frame is measured with a 16 bit encoder, and controlled with a linear actuator.

Absolute pointing is determined with star cameras taking images at the ends of each scan. In order to determine the pointing along the scan, the platform’s angular velocity around three orthogonal axes is measured with fiber optic gyroscopes. These velocities are then integrated with respect to time to determine the position relative to the end point of the scan. Pointing reconstruction is better than 10 arc-sec at all points along the scan. Redundancy in the absolute pointing determination is provided by a sun sensor, differential GPS, and a three axis magnetometer.

The warm optics consist of a reflecting Gregorian Dragone telescope with a field of view of six degrees. The primary and secondary mirrors are both aluminium. The cold optics are shown in the cut-away diagram of the cryostat in Figure 6. The lenses are all AR coated Ultra High Molecular Weight Polyethylene. The cryostat contains a liquid helium bath held at atmospheric pressure, surrounded by a liquid nitrogen bath and vapour cooled shields. The designed hold time of the cryostat is 21 days. The detectors are cooled to less than 300mK using a ^3He adsorption refrigerator.

The two focal planes are hexagonal arrays of conical smooth-bore horns, optically coupled to bolometers. The bolometers are transition edge sensitive (TES) devices²⁴. The expected noise equivalent power (NEP) of a single bolometer is $3.8 \times 10^{-17} \text{W}/\sqrt{\text{Hz}}$. This is the quadrature sum of the (dominant) phonon noise and TES Johnson noise. Band defining filters are held above the horns. Figure 7 shows a cut-away diagram of one of the two focal planes, with different colours representing different frequency bands.

Detector readout is performed by a new low-power digital frequency multiplexing scheme^{23,27}. The readout noise of the system (not including TES noise) is measured as $1.9 \times 10^{-18} \text{W}/\sqrt{\text{Hz}}$, lower than the expected noise from the bolometer. The power utilization for the LD flight is estimated at 550 W. This low power draw allows for a large number of detectors on a power limited system like a balloon platform.

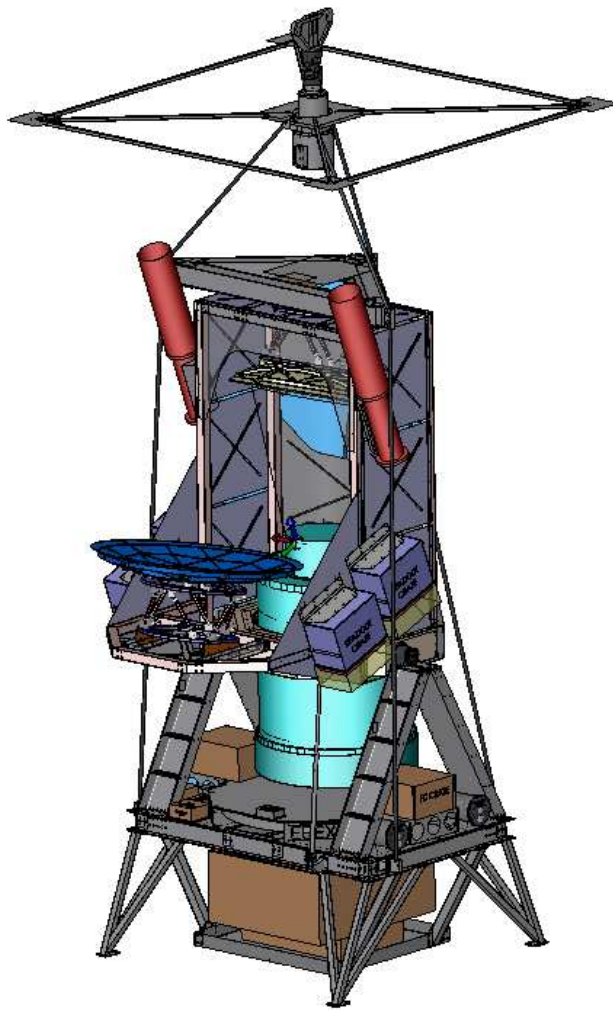


Figure 5: The *EBEX* gondola without sun shields or solar panels.

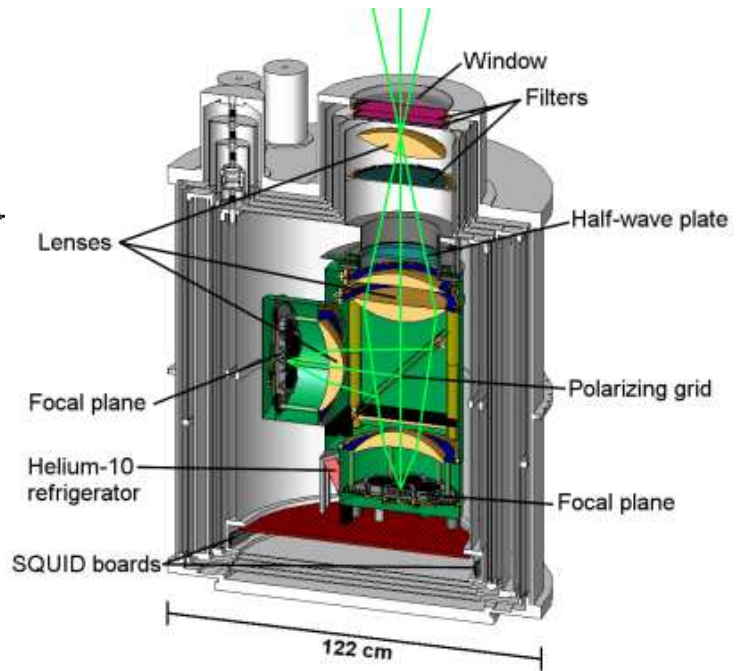


Figure 6: Internal view of the cryostat.

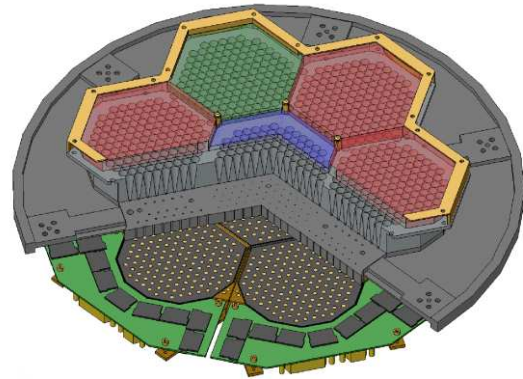


Figure 7: One of the two *EBEX* focal planes. The red hexagons are the 150GHz detectors, green are 250GHz detectors and the central blue hexagon contains the 410GHz detectors. The TES wafers are shown in gray and yellow.

Polarimetry is performed with an achromatic half wave plate (HWP) continuously rotated at 6 Hz in the Lyot-stop of the cold optics. The achromatic half wave plate is made by stacking 5 chromatic sapphire HWPs, each 1.62 mm thick, at orientations of (0, 25, 85, 25, 0) $^\circ$ relative to the crystal axis of the first. The HWP is AR coated with expanded Teflon. The HWP is driven continuously via a Kevlar belt and is supported by a superconducting magnetic bearing operating at 4 K²⁶. Superconducting bearings are suitable for this application because they can have friction that are smaller than the friction of standard bearings by a factor of up to 10,000, decreasing heat load and increasing cryogen hold time.

5 Conclusion

We have discussed the design of *EBEX*, a balloon borne CMB polarization experiment. *EBEX* is designed to detect or constrain the amplitude of B-modes, probing the exponential expansion of the universe. In addition, *EBEX* will make cosmic variance limited measurements of the E-modes from $16 < l < 1500$.

Acknowledgments

EBEX is a NASA supported mission through grant number NNX08AG40G. We also acknowledge support from the Canadian Institute for Advanced Research, CNRS, Minnesota Supercomputing Institute, NSF GK-12 grant 0638688, Rhode Island Space Grant, and the Science and Technology Facilities Council. This research used resources of the National Energy Research Scientific Computing Center, which is supported by the Office of Science of the U.S. Department of Energy under Contract No. DE-AC02-05CH11231. CB was supported in part by the NASA LTSA Grant NNG04CG90G, and BJ acknowledges a PPARC Postdoctoral Fellowship and NSF IRFP Fellowship.

References

1. A.H. Guth, *Phys. Rev. D* **23**, 347 (1981).
2. A.D. Linde, *Phys. Lett. B* **108**, 389 (1982).
3. A. Albrecht and P. J. Steinhardt, *Phys. Rev. Lett.* **48**, 1220 (1982).
4. K. Sato, *MNRAS* **195**, 467 (1981).
5. J. Dunkley, *et al*, astro-ph 0803.0586.
6. M. Tegmark *et al*, *Phys. Rev. D* **74**, 123507 (2006).
7. E.W. Kolb and M.S. Turner in *The Early Universe*, (Addison-Wesley, CA, 1994).
8. A.A. Starobinsky, *Phys. Lett. B* **117**, 175 (1982).
9. A. A. Starobinskii, *Soviet Astro Lett* **9**, 302 (1983).
10. V.A. Rubakov *et al*, *Phys. Lett. B* **115**, 189 (1982).
11. L.P. Grishchuk, *Sov Phys. JETP* **40**, 409 (1975).
12. L. F. Abbott and M. B. Wise, *Nuclear Physics B* **244**, 541 (1984).
13. M.Kamionkowski *et al*, *Phys. Rev. D* **55**, 7368 (1997).
14. U. Seljak and M. Zaldarriaga, *Phys. Rev. Lett.* **78**, 2054 (1997).
15. M.Kamionkowski *et al*, *Phys. Rev. Lett.* **78**, 2058 (1997).
16. M.Zaldarriaga and U.Seljak., *Phys. Rev. D* **55**, 1830 (1997).
17. D. Ball (NSBF Head of Operations), 2004. Private communication.
18. J.Bock *et al*, Task force on cosmic microwave background research, 2006.
19. U.Seljak, *ApJ* **482**, 6 (1997)
20. M.Zaldarriaga and U.Seljak, *Phys. Rev. D* **58**, 23003 (1998).
21. E. Komatsu, *et al*, astro-ph 0803.0547v1.
22. M.Tegmark, *et al*, *Phys. Rev. D* **69**, 103501 (2004).
23. M.Dobbs, *et al*, *Proc SPIE NPSS Real Time Conf.*
24. S.Lee, *et al*, *Appl. Optics* **37**, 3391 (1998)
25. R.Stompor, *et al* astro-ph 0804.2645, (2008)
26. S.Hanany, *et al* *IEEE Applied Superconductivity* **13**, 2128 (2003).
27. J.Hubmayr, *et al*, *Proc SPIE Astro.Inst.*